

Original Research

FOXA1/UBE2T Inhibits CD8⁺T Cell Activity by Inducing Mediates Glycolysis in Lung Adenocarcinoma

Jiangtao Pu^{1,*}, Dengguo Zhang¹, Biao Wang¹, Peiquan Zhu¹, Wenxing Yang¹,
Kaiqiang Wang¹, Ze Yang¹, Qi Song¹¹Department of Thoracic Surgery, Affiliated Hospital of Southwest Medical University, 646000 Luzhou, Sichuan, China*Correspondence: drjiangtaop@163.com (Jiangtao Pu)

Academic Editor: Roberto Bei

Submitted: 25 August 2023 Revised: 23 November 2023 Accepted: 5 January 2024 Published: 1 April 2024

Abstract

Background: Immune escape is a key factor influencing survival rate of lung adenocarcinoma (LUAD) patients, but molecular mechanism of ubiquitin binding enzyme E2T (UBE2T) affecting immune escape of LUAD remains unclear. The objective was to probe role of UBE2T in LUAD. **Methods:** Bioinformatics means were adopted for analyzing UBE2T and forkhead box A1 (FOXA1) expression in LUAD tissues, the gene binding sites, the pathway UBE2T regulates, and the correlation between UBE2T and glycolysis genes. Dual luciferase and chromatin immunoprecipitation (ChIP) assays were conducted for validating the binding relationship between the two genes. Quantitative reverse transcription polymerase chain reaction (qRT-PCR) and western blot were employed to evaluate UBE2T, FOXA1, and programmed death ligand 1 (PD-L1) levels in cancer cells. MTT assay was conducted for detecting cell viability. Cytotoxicity assay detected CD8⁺T cell toxicity. Cytokine expression was assayed by enzyme linked immunosorbent assay (ELISA). Extracellular acidification rate (ECAR) and oxygen consumption rate (OCR) were assayed by extracellular flow analyzer. Glycolytic gene expression was analyzed by qRT-PCR, and glycolysis-related indicators were detected by ELISA. Immunohistochemistry (IHC) detected CD8⁺T cell infiltration in tumor tissues. **Results:** FOXA1 and UBE2T were up-regulated in LUAD, and a binding site existed between UBE2T and FOXA1. Overexpressing UBE2T could increase PD-L1 expression and inhibit toxicity of CD8⁺T cells to LUAD cells. Overexpressing UBE2T repressed CD8⁺T cell activity in LUAD by activating the glycolysis pathway, and the addition of glycolysis inhibitor 2-deoxy-d-glucose (2-DG) reversed the above results. Mechanistically, FOXA1 promoted the immune escape of LUAD by up-regulating UBE2T and thus mediating glycolysis. *In vivo* experiments revealed that UBE2T knockdown hindered tumor growth, inhibited PD-L1 expression, and facilitated CD8⁺T cell infiltration. **Conclusion:** FOXA1 up-regulated the expression of UBE2T, which activated glycolysis, and thus inhibited activity of CD8⁺T cells, causing immune escape of LUAD.

Keywords: FOXA1; UBE2T; glycolysis; lung adenocarcinoma; CD8⁺T cells

1. Introduction

Currently, lung cancer is implicated in an unsatisfactory prognosis [1]. Among lung cancers, proportion of non-small cell lung cancer (NSCLC) is about 80%, and most of the NSCLCs are lung adenocarcinomas (LUADs) [2,3]. In recent years, reversing effector T cell failure by immune checkpoint blocking with reagents such as programmed cell death protein 1 (PD-1) and programmed death ligand 1 (PD-L1) antibodies is a regular method for lung cancer [4]. However, a sizable percentage of patients did not respond to these manipulations, partly due to immune escape of tumor cells during contact with immune cells in microenvironment. Hence, exploring the mechanism of immune evasion is a necessary way to improve patient's survival rate and can bring a new choice for the precise treatment of LUAD.

The process by which tumor cells avoid immune system monitoring and use various strategies to facilitate their migration and invasion is known as tumor immune escape [5]. PD-L1 shows a critical role in keeping immune homeostasis, in which PD-L1 on tumor cell surface interplays with PD-1 in T cells to inhibit T lymphocyte activation,

and cytokine secretion [6]. In the tumor microenvironment (TME), this approach is adopted by cancer cells to avoid T-cell-mediated tumor-specific immunity [6]. Numerous studies have investigated the mechanism by which PD-L1 influences activity of CD8⁺T cells. Liu *et al.* [7] manifested that N⁶-methyladenosine-modified circIGF2BP3 represses CD8⁺T cell activity by driving PD-L1 deubiquitination in NSCLC, promoting tumor immune escape. CircRNA CHST15 sponges, miR-155-5p and miR-194-5p, facilitate PD-L1-mediated immune evasion in lung cancer [8]. In spite of this, the molecular mechanism mediating the immune escape of LUAD has not been completely clarified. The present study will continue to search for molecular targets that can inhibit CD8⁺T cell activity by influencing PD-L1 expression, offering novel ideas for research and development of therapies for LUAD.

Metabolic reprogramming is a signature of cancer [9]. Aerobic glycolysis, namely "Warburg effect", is the most commonly seen mode of metabolic reprogramming and also the common way for cancer cells to metabolize glucose [10]. Somatic cells synthesize adenosine triphos-



phate (ATP) by oxidative phosphorylation, while tumor cells generate lactic acid by glycolysis [11]. Numerous reports supported the view that glycolysis regulates tumor development. As a study shows, succinate dehydrogenase B (SDHB) hinders occurrence and development of renal clear cell carcinoma by inhibiting glycolysis [12]. According to Zhao *et al.* [13], lncRNA MIR17HG facilitates colorectal cancer liver metastasis by mediating a positive feedback loop related to glycolysis. Furthermore, glycolysis metabolism was found to be associated with PD-L1-mediated immune evasion in TME of malignant tumors [14]. Glucose metabolism reprogramming drives immune evasion in hepatocellular carcinoma and pancreatic cancer [15,16]. For example, high glucose stimulates pancreatic cancer cells to evade immune surveillance through the AMPK-Bmi1-GATA2-MICA/B pathway [17]. However, it is not clear how glycolytic metabolism in LUAD regulates tumor immune escape.

Ubiquitin binding enzyme E2T (UBE2T) is a representative E2 containing UBC domain that can link to ring finger or HECT domain of E3 and promotes monoubiquitination or poly-ubiquitination of substrates [18]. Accumulating evidence shows that UBE2T exerts a carcinogenic effect in varying cancers and is closely linked to cancer occurrence and progression, including hepatocellular carcinoma [19], gastric cancer [20], and multiple myeloma [21]. The function of UBE2T in development of lung cancer has also been investigated. For example, UBE2T up-regulates the autophagy of NSCLC cells through activating the p53/AMPK/mTOR pathway [18]. UBE2T promotes radiation resistance of NSCLC through driving epithelial-mesenchymal transition (EMT) and FOXO1 degradation mediated by ubiquitination [22]. In addition, UBE2T level is linked to infiltration of immune cells. For example, Wang *et al.* [23] disclosed that UBE2T level is substantially increased in retinoblastoma and is positively correlated with Th2 cells, acting as a prognostic biomarker for retinoblastoma. Similarly, survival analysis presented that UBE2T is increased in breast cancer, and its up-regulation is linked with unfavorable prognosis. UBE2T up-regulation is linked to Th1 and Th2 cell balance, and Th1/Th2 balance shifts to Th2 in basal and Luminal-B breast cancer ($p < 0.05$) [24]. Despite these interesting findings, immunosuppressive function of UBE2T in LUAD is largely unclear. Therefore, this work continued to delineate mechanism by which UBE2T modulated activity of CD8⁺T cells in LUAD, with a view of providing a theoretical basis for searching new LUAD treatment strategies.

One pioneer factor that can bind to concentrated chromatin and start chromatin remodeling is the forkhead box A1 (FOXA1) protein [25]. Target genes are transcriptionally activated when FOXA1 interacts to its co-factors. FOXA1 mutations are a defining characteristic of estrogen receptor-positive (ER) breast cancer and contribute to the disease advancement through estrogen receptor-binding

events [26]. When combined with HOXB13, FOXA1 can cause normal prostate epithelial cells to undergo a transformation [27]. SOX9 up-regulates FOXA1 and drives tumorigenic potential of lung cancer cells [28]. Thus, targeted interference with FOXA1 may serve as a substitute approach for LUAD therapy.

In this work, we focused on clarifying function of UBE2T in LUAD. As our results displayed, UBE2T was increased in LUAD tissues and cells and repressed activity of CD8⁺T cells in LUAD through glycolysis pathway. Additionally, FOXA1 was an upstream transcription factor for UBE2T and regulated the expression of UBE2T. Subsequently, we verified through cell and animal experiments that the FOXA1/UBE2T axis inhibited CD8⁺T cell activity in LUAD via the glycolysis pathway. Our findings prefer experimental evidence for explaining molecular mechanism of LUAD immune escape and novel targets for LUAD treatment.

2. Materials and Methods

2.1 Bioinformatics Analysis

mRNA expression data (59 normal cases, 539 tumor cases) of LUAD were downloaded from The Cancer Genome Atlas (TCGA) and subjected to differential analysis ($|\log_{2}FC| > 1.0$, false discovery rate (FDR) < 0.05), which was carried out by the “edgeR” package 4.2.3 (Posit, Boston, MA, USA), to get differentially expressed mRNAs (DEmRNAs) between normal and tumor groups. Then, by combining with the literature [29], the target gene for the study was determined. Next, the pathways regulated by target gene were predicted through gene set enrichment analysis (GSEA, $|NES| > 1.0$, FDR < 0.25), and transcription factors upstream of target gene were predicted by TFtarget. Intersection of transcription factors from prediction and DEmRNAs was obtained by overlapping and visualized by the upset plot generated by the R package “UpSetR” (<http://github.com/hms-dbmi/UpSetR>). Pearson correlation analysis was conducted between obtained transcription factors and target gene, and the transcription factor with a higher correlation was selected as the research object. JASPAR was utilized to predict motif binding site at 2000 bp upstream of target gene. The immune infiltration data of all tumor samples of TCGA were accessed from Timer2.0 (<http://timer.comp-genomics.org/timer/>), and the expression matrices of UBE2T in TCGA samples were integrated with the expression matrices of individual immune cells using various algorithms such as TIMER, CIBERSORT, CIBERSORT-ABS, QUANTISEQ, MCPOUNTER, XCELL, and EPIC and other algorithms to compute immune cell infiltration in TCGA samples, integrate expression matrix of UBE2T in TCGA-LUAD samples with the infiltration matrix of individual immune cells, and conduct Pearson correlation analysis.

2.2 Cell Culture

Human lung bronchial epithelial cells (BEAS-2B), LUAD cells (A549, H460, and H1650), 293T cells, and peripheral blood mononuclear cells (PBMCs) were purchased from ATCC (Manassas, VA, USA), and mouse LUAD cells (LA795) were purchased from Pricella (Wuhan, China). BEAS-2B cells were maintained in MEM with 10% fetal bovine serum (FBS; PAN, Aidenbach, Germany), A549 cells in F12K medium (Invitrogen, Waltham, MA, USA) containing 10% FBS (PAN, Germany), H460 cells and H1650 cells in RPMI-1640 medium (Invitrogen, Waltham, MA, USA) with 10% FBS (PAN, Germany), 293T cells in DMEM (Invitrogen, Waltham, MA, USA) with 10% FBS (PAN, Germany) and 2 mM L-glutamine (Invitrogen, Waltham, MA, USA), and PBMC cells in HBSS medium (Invitrogen, Waltham, MA, USA) containing 10% FBS (PAN, Germany). LA795 cells were placed in RPMI-1640 culture-medium (Invitrogen, Waltham, MA, USA) mixed with 10% FBS (PAN, Germany), streptomycin (100 µg/mL, Corning, Shanghai, China), penicillin G (100 U/mL, Beyotime, Shanghai, China). The cultured cells were incubated in humidified atmosphere with 5% CO₂ at 37 °C. All cell lines were validated by STR profiling and tested negative for mycoplasma. Glycolysis inhibitor 2-deoxy-d-glucose (2-DG) was purchased from Warbio (Nanjing, China).

2.3 Cell Transfection

Short hairpin RNAs (shRNAs) targeting UBE2T and FOXA1 (sh-UBE2T, sh-FOXA1) and their negative controls (sh-NC) were produced by GenePharma (Shanghai, China), and the carrier pcDNA-UBE2T and its negative control pcDNA-NC were accessed from RiboBio (Guangzhou, China). As per the instructions, sh-UBE2T, sh-FOXA1, sh-NC, pcDNA-UBE2T, and pcDNA-NC were used to transfect LUAD cells using Lipofectamine 2000 (Invitrogen, Waltham, MA, USA).

2.4 Quantitative Reverse Transcription Polymerase Chain Reaction (qRT-PCR)

Total RNA extraction from tissues and cells was conducted by using TRIzol reagents (Invitrogen, Waltham, MA, USA), and RNA concentration and purity were quantitatively determined with a NanoDrop ND-1000 spectrophotometer (NanoDrop, Waltham, MA, USA). Revert Aid™ First Strand cDNA Synthesis Kit (Thermo Fisher, Waltham, MA, USA) was applied to synthesize cDNA from RNA. ChamQ SYBR Color qPCR Master Mix (High ROX Premixed; Vazyme, Nanjing, China) was utilized to perform qPCR on ABI 7500 PCR instrument (Applied Biosystems, Waltham, MA, USA). Total reaction volume was 20 µL. Relative expression of genes was computed by applying $2^{-\Delta\Delta CT}$. β -actin gene was taken as a control. Sequences of primers are listed in Table 1.

2.5 MTT

(3-(4,5-Dimethylthiazol-2-yl)-2,5-Diphenyltetrazolium Bromide) Assay

LUAD cells were inoculated into 96-well plates (1×10^3 cells/well). After incubation at 37 °C for 0, 24, 48, and 72 h, medium was replaced and 20 µL MTT reagent was introduced (5 mg/mL; Sigma-Aldrich, St. Louis, MO, USA). After culture at 37 °C for 4 h, supernatant was discarded and 200 µL DMSO (Invitrogen, Waltham, MA, USA) was introduced. Absorbance at 570 nm was obtained by a microplate reader (Varioskan LUX, Invitrogen, Waltham, MA, USA).

2.6 Western Blot Analysis

Total protein extraction from tissues and cells was performed with RIPA buffer (Sigma, St. Louis, MO, USA), followed by protein concentration determination by a BCA protein detection kit (Thermo Fisher, Waltham, MA, USA). SDS-PAGE was run for protein isolation with 10% polyacrylamide gel (Beyotime, Shanghai, China) and transferred to a polyvinylidene fluoride membrane (Beyotime, Shanghai, China). Thereafter, membrane was incubated with primary antibodies (Abcam, Cambridge, UK) of the proteins PD-L1 (1:1000), UBE2T (1:1000), GLUT1 (1:100,000), LDHA (1:5000), HK2 (1:1000) and FOXA1 (1:5000) overnight. The next step was incubation for 1 h with second antibody IgG (Abcam, Cambridge, UK) at room temperature. β -actin acted as a control, and a rabbit anti- β -actin antibody (Abcam, Cambridge, UK) was adopted. Protein bands were developed after the introduction of an ECL-based chemiluminescence substrate (Millipore, Burlington, MA, USA).

2.7 Extraction of CD8⁺T Cells and Co-Culture of CD8⁺T Cells with LUAD Cells

T cells were purified from PBMCs using magnetic beads from Miltenyi Biotech (Bergisch Gladbach, North Rhine-Westphalia, Germany). Then, CD8⁺T cells were activated by the addition of IL-2 (10 IU/mL, Abcam, Cambridge, UK), anti-CD3 (2.5 µg/mL; Abcam, Cambridge, UK), and anti-CD28 (2 µg/mL, Abcam, Cambridge, UK) [30]. Afterward, treated LUAD cells were mixed with activated CD8⁺T cells (the ratio of reactive agent to the stimulus was 1:1). They were then maintained in RPMI-1640 medium, which contained 10 mM HEPES, 10% heat-inactivated FBS, 100 ng/mL streptomycin and 100 U/mL penicillin, for 96 h [31].

2.8 CD8⁺T Cytotoxicity Test

CD8⁺T cell cytotoxicity was assayed with lactate dehydrogenase (LDH) cytotoxicity kit (Thermo Fisher, Waltham, MA, USA). Cytotoxicity was measured following: Cytotoxicity% = [(Chemical-treated LDH activity – Spontaneous LDH activity)/(Maximum LDH activity – Spontaneous LDH activity)] × 100% [32].

Table 1. Primers for quantitative reverse transcription polymerase chain reaction (qRT-PCR).

Primer	Forward (5'-3')	Reverse (5'-3')
<i>UBE2T</i>	ATCCCTCAACATCGCAACTGT	CAGCCTCTGGTAGATTATCAAGC
<i>LDHA</i>	TGGAGATTCCAGTGTGCCTGTATGG	CACCTCATAAGCACTCTCAACCACC
<i>GLUT1</i>	CTTTGTGGCCTTCTTTGAAGT	CCACACAGTTGCTCCACAT
<i>HK2</i>	GAGCCACCACTCACCTACT	CCAGGCATTGGCAATGTG
<i>FOXA1</i>	ACAGCTACTACGCAGACACG	ACAGCTACTACGCAGACACG
<i>β-actin</i>	CTACGTCGCCCTGGACTTCGAGC	GATGGAGCCGCCGATCCACACGG

UBE2T, ubiquitin binding enzyme E2T; GLUT1, glucose transporter type 1; LDHA, lactate dehydrogenase A; HK2, hexokinase 2; FOXA1, forkhead box A1.

2.9 Enzyme Linked Immunosorbent Assay (ELISA)

Interferon γ (IFN γ), tumor necrosis factor α (TNF α), and interleukin (IL) 2 levels were tested with ELISA kits (Abcam, Cambridge, UK). In short, supernatant of each co-culture group was harvested. Next, each sample well was added with 100 μ L enzyme conjugate and allowed for reaction at 37 °C for 30 min. Then, each well was introduced with 100 μ L horseradish peroxidase substrate solution for color development at 37 °C for 20 min. Lastly, each well was added with 50 μ L termination solution and the absorbance at 450 nm was assessed within 20 min [32].

2.10 Detection of Oxygen Consumption Rate (OCR) and Extracellular Acidification Rate (ECAR)

We measured cellular glycolysis capacity and mitochondrial function by extracellular flow analyzer (Seahorse Bioscience, North Billerica, MA, USA) as per instructions. The day before assay, cells were placed in cell culture microporous boards (Seahorse Bioscience, North Billerica, MA, USA). Seahorse buffer was a mixture of DMEM, 2 mM sodium pyruvate, phenol red, 25 mM glucose, and 2 mM glutamine. For ECAR value test, 10 mM glucose, 1 μ M oligomycin, and 100 mM 2-DG were automatically added. Following baseline respiration monitoring, 1 μ M oligomycin, 1 μ M carbonyl cyanide 4-(trifluoromethoxy)phenylhydrazone (FCCP), and 1 rotenone were automatically injected into the microporous boards to assess OCR [1].

2.11 Dual Luciferase Assay

The fragment of UBE2T was inserted into pGL3 promoter vector to construct pGL3-UBE2T-promoter-WT (wild type) or pGL3-UBE2T-promoter-MUT (mutation type) vector. The luciferase reporter vector and sh-FOXA1/sh-NC were used for co-transfection of 293T cells by Lipofectamine 2000 reagent. The 293T cells were incubated for 48 h, followed by luciferase activity measurement in dual luciferase assay system.

2.12 Chromatin Immunoprecipitation (ChIP) Assay

After 37% formaldehyde (Beyotime, Shanghai, China) treatment, the cells were collected for sonica-

tion with VCX750 (SONICS, Newtown, CT, USA) at 25% power. Sonication was performed for 4.5 s each time, with 14 times in total and 9 s intervals. Next, centrifugation at 10,000 \times g was performed at 4 °C for 10 min, and insoluble matter was discarded. Then, an antibody against FOXA1 (Abcam, Cambridge, UK) and a control IgG antibody (Abcam, Cambridge, UK) were introduced to bind to target protein-DNA complex. Then, protein A was applied to sediment antibody-target protein-DNA complex. After washing the sediment, the sediment was eluted and de-crosslinked. Finally, the purified DNA sequences were used for qPCR [33]. PCR primer sequences were as follows: forward direction, 5'-AGTGAACATCTGGGTTGGTAAA-3' and reverse direction, 5'-AGTGAACATCTGGGTTGGTAAA-3'.

2.13 Immunohistochemistry (IHC) Assay

The paraffin-embedded sample was sliced into 4 μ m-thick slices using a paraffin microtome (Leica, Wetzlar, Germany). IHC staining was completed according to the standard protocol described previously [18]. After initial dewaxing, antigen repair, and sealing, the slices were incubated overnight with anti-UBE2T antibody (Abcam, Cambridge, UK) in a humid container at 4 °C. The next day, slices were treated with horseradish peroxidase-labeled secondary antibody IgG (Abcam, Cambridge, UK). DAB (Novus Biologicals, Littleton, CO, USA) was adopted to develop UBE2T staining, and hematoxylin counterstaining was conducted.

2.14 Establishment of Allograft Model

Thirty male mice (BALB/c, 4 weeks old, 18–22 g) were from SLAC Laboratory Animal Co., Ltd. (Shanghai, China). Animal experiments were conducted with approval from the Ethics Committee of Affiliated Hospital of Southwest Medical University. Mice were kept in controlled conditions with 25 ± 2 °C, a humidity of 70%, a light-dark cycle of 12 h, and regular food and water feeding. LA795 cells (1×10^5) with sh-NC or sh-UBE2T were subcutaneously inoculated into the right flank of each mouse. The formula of $V(\text{volume}) = W(\text{width})^2 \times L(\text{length})/2$ was adopted for calculating tumor volume, and mice were weighed every 5

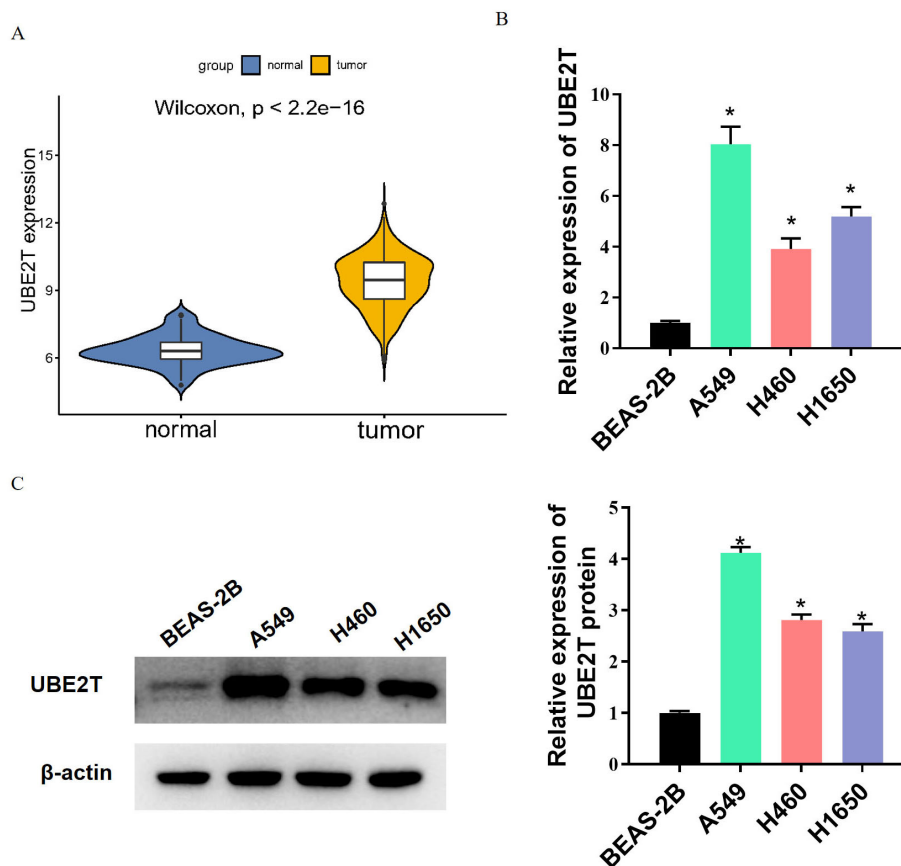


Fig. 1. UBE2T expression is up-regulated in LUAD. (A) UBE2T expression in LUAD tissues analyzed by bioinformatics approaches. (B,C) Expression of UBE2T in LUAD cells analyzed by western blot and qRT-PCR. * indicates $p < 0.05$. UBE2T, ubiquitin binding enzyme E2T; LUAD, lung adenocarcinoma; qRT-PCR, quantitative reverse transcription polymerase chain reaction.

days. On day 30, mice were euthanized, and tumor weight was measured. Tumor tissues were collected from each group and the tumor growth was measured.

2.15 Statistical Analysis

Data were processed using GraphPad Prism 8.0 (GraphPad Software, Inc., San Diego, CA, USA). All measured data were presented in the form of mean \pm standard deviation (SD). *T*-test was applied for detecting differences between two groups. Each experiment was conducted at least three times. $p < 0.05$ indicated a significant difference.

3. Results

3.1 UBE2T Is Up-Regulated in LUAD

Previous studies have found that UBE2T is up-regulated and promotes cancers of various types, such as hepatocellular carcinoma [34] and esophageal squamous cell carcinoma [35]. Hence, we explored UBE2T expression in LUAD. Bioinformatics results showed a significant up-regulation of UBE2T in LUAD tissues (Fig. 1A). qRT-PCR and western blot detection also showed an evident higher UBE2T expression in LUAD cells than in normal

lung epithelial cells (Fig. 1B,C). These results suggested the aberrantly high expression of UBE2T in LUAD. Since UBE2T had higher relative expression in A549 cells and lower expression in H460 cells among the tested cell lines, A549 was selected for the subsequent knockdown experiment and H460 for the overexpression experiment.

3.2 High Expression of UBE2T Inhibits the Activity of CD8⁺T Cells

UBE2T is associated with immune cell infiltration [24]. We found by bioinformatics analysis that UBE2T had a negative correlation with CD8⁺T cell infiltration (Fig. 2A). The following cell lines were constructed: sh-NC, sh-UBE2T, oe-NC, and oe-UBE2T. As qRT-PCR and MTT results revealed, sh-UBE2T substantially reduced UBE2T expression and cell viability, while oe-UBE2T significantly increased UBE2T expression and cell viability (Fig. 2B,C). The above cells were co-cultured with activated CD8⁺T cells separately. Western blot showed down-regulated PD-L1 expression after sh-UBE2T treatment and up-regulated PD-L1 expression after oe-UBE2T treatment (Fig. 2D). In addition, after sh-UBE2T treatment, CD8⁺T cells showed enhanced toxicity to A549 cells and increased

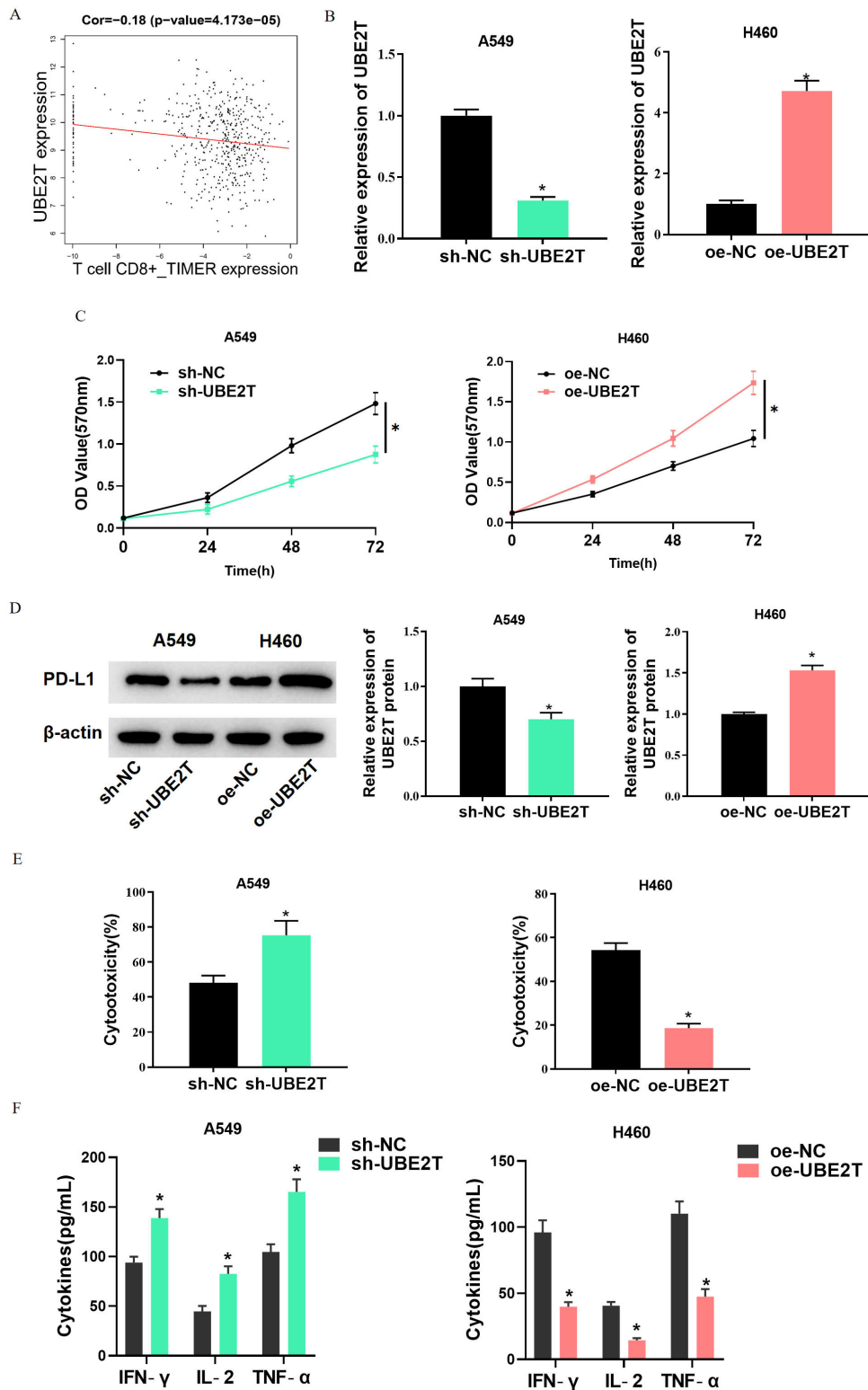


Fig. 2. High expression of UBE2T inhibits the activity of CD8⁺T cells. (A) Bioinformatics analysis on correlation between UBE2T and CD8⁺T cell infiltration. (B) qRT-PCR analysis on UBE2T expression in LUAD cells after knockdown and overexpression. (C) MTT assay results on LUAD cell activity after knockdown and overexpression. (D) Western blot analysis on PD-L1 expression. (E) LDH toxicity assay on cytotoxicity of CD8⁺T cells co-cultured with LUAD cells. (F) ELISA results on the expression of cytokines. * indicates $p < 0.05$. ELISA, enzyme linked immunosorbent assay; PD-L1, programmed death ligand 1; MTT, 3-(4,5-dimethylthiazol-2-yl)-2,5-diphenyltetrazolium bromide; LDH, Lactate dehydrogenase; sh, short hairpin RNA; oe, overexpression; NC, negative control; OD, optical density; IFN- γ , Interferon- γ ; IL-2, interleukin-12; TNF- α , tumor necrosis factor- α .

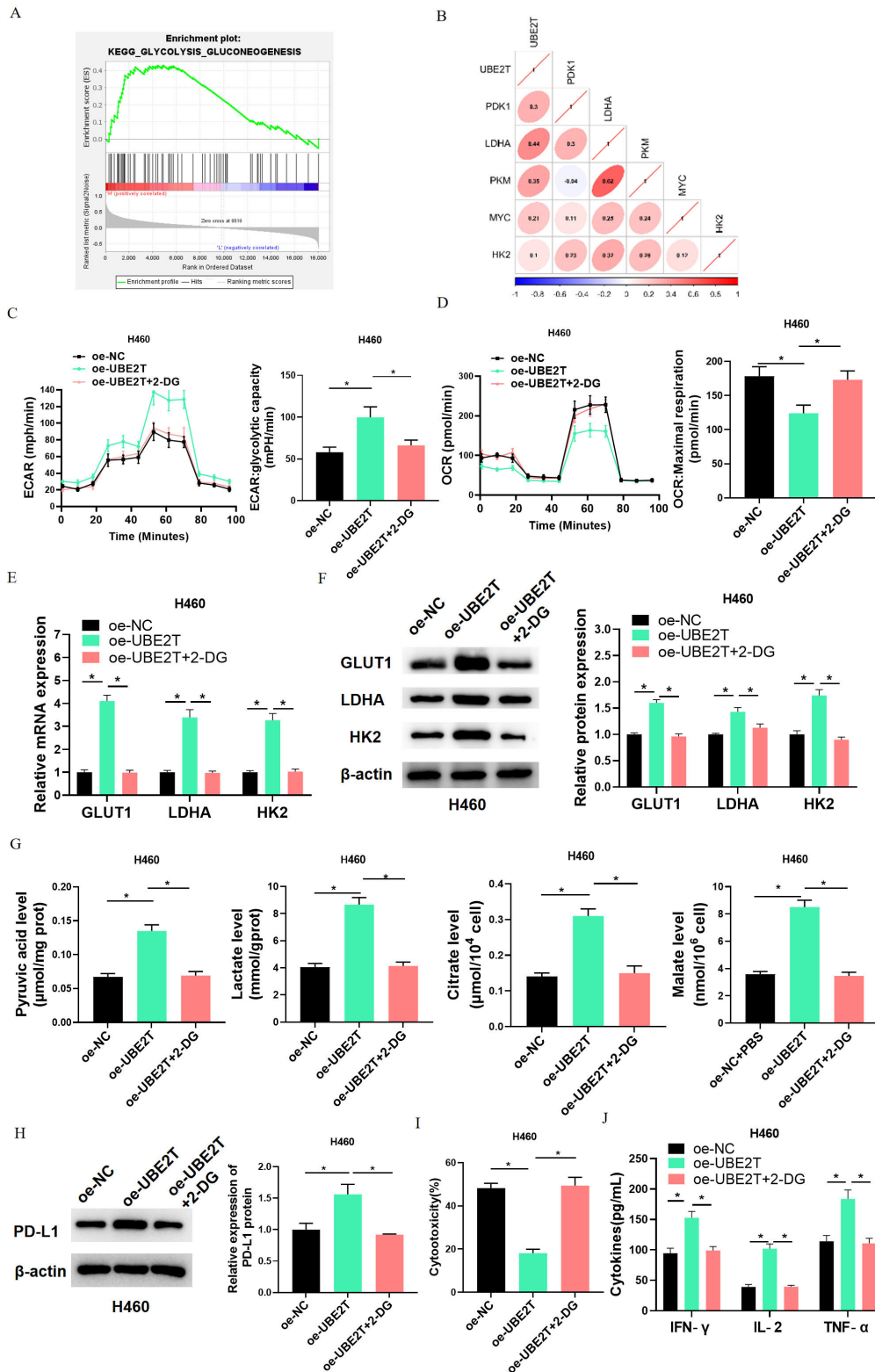


Fig. 3. High expression of UBE2T inhibits CD8⁺T cell activity by activating glycolysis. (A) Bioinformatics analysis results of UBE2T enrichment pathway. (B) Pearson correlation analysis of UBE2T and glycolytic related genes. (C,D) Determination of ECAR and OCR of H460 cells after different treatments. (E,F) qRT-PCR and western blot analysis results of expression of glycolysis-related genes after different treatments. (G) Contents of pyruvate, lactic acid, citric acid and malic acid in H460 cells after different treatments. (H) Western blot analysis results of PD-L1 expression. (I) Cytotoxicity assay results of CD8⁺T cell cytotoxicity to H460 cells. (J) ELISA detection results on cytokine expression. * indicates $p < 0.05$. ECAR, extracellular acidification rate; OCR, oxygen consumption rate; 2-DG, 2-deoxy-d-glucose.

expression of cytokines (IFN- γ , IL-2, TNF- α), while after oe-UBE2T treatment, CD8⁺T cells showed reduced toxicity to H460 cells and decreased expression of cytokines (Fig. 2E,F). The above experiments demonstrated that high UBE2T expression in LUAD hindered CD8⁺T cell activity.

3.3 High Expression of UBE2T Inhibits CD8⁺T Cell Activity by Activating Glycolysis

Next, we investigated mechanism that UBE2T affects activity of CD8⁺T cells in LUAD. As we found, UBE2T was divided into two groups based on UBE2T expression: UBE2T-high and UBE2T-low. Single gene GSEA presented that UBE2T was highly expressed in the glycolysis signaling pathway (normalized enrichment scores (NES) = 1.51, FDR = 0.141) (Fig. 3A, **Supplementary Table 1**), and its expression was positively correlated with genes related to glycolysis (Fig. 3B). We hypothesized that UBE2T high expression could inhibit CD8⁺T cell activity through the glycolysis pathway. To verify this conjecture, we constructed the following cell lines based on H460 cells: oe-NC (oe-NC+DMSO), oe-UBE2T (oe-UBE2T+DMSO), and oe-UBE2T+2-DG. Seahorse XF extracellular flow analyzer was applied for analyzing the effect of abnormal UBE2T expression on glycolysis. ECAR reflects aerobic glycolysis flux, and OCR demonstrates mitochondrial oxidative respiration state. As our results displayed, the ECAR level was notably increased in H460 cells with UBE2T overexpression, reflecting that UBE2T overexpression could promote glycolysis level, while the addition of 2-DG restored ECAR value to the control level (Fig. 3C). Cellular oxygen consumption indicates mitochondrial respiration level, and OCR decreases when aerobic glycolysis occurs. In contrast to ECAR results, we observed that UBE2T overexpression reduced OCR level in H460 cells, but this was reversed by the addition of 2-DG (Fig. 3D). Expression of glycolysis-related genes was analyzed by qRT-PCR and western blot. Overexpression of UBE2T significantly enhanced GLUT1, LDHA and HK2 expression, but 2-DG reversed this result (Fig. 3E,F). Then, we tested contents of pyruvate, lactic acid, citric acid, and malic acid in cells in each group using corresponding kits. The results were that these contents in cells increased after oe-UBE2T treatment, while these indicators were reversed by 2-DG treatment (Fig. 3G). In conclusion, UBE2T positively regulated aerobic glycolysis in LUAD cells.

Next, H460 cells with oe-NC, oe-UBE2T, or oe-UBE2T+2-DG were subjected to co-culture with activated CD8⁺T cells. As western blot showed, UBE2T overexpression could largely increase PD-L1 expression, but the addition of 2-DG restored PD-L1 to the control level (Fig. 3H). According to cytotoxicity test results, CD8⁺T cytotoxicity to H460 cells was weakened after UBE2T overexpression, and impact of UBE2T overexpression on CD8⁺T cell cytotoxicity was counteracted after 2-DG was added (Fig. 3I). ELISA showed similar results in terms of the expression

of related cytokines. Overexpression of UBE2T resulted in decreased levels of cytokines (IFN- γ , IL-2, TNF- α), but this was reversed by the addition of 2-DG (Fig. 3J). In conclusion, high expression of UBE2T in LUAD could repress CD8⁺T activity by promoting glycolysis levels.

3.4 FOXA1 Activates UBE2T Transcription

To explore the transcription factors upstream of UBE2T, hTFtarget was utilized to predict UBE2T upstream potential transcription factors, which were then intersected with up-regulated DEmRNAs. Finally, a total of 17 potential transcription factors were obtained (Fig. 4A). FOXA1 is associated with the growth and cell characteristics of LUAD [36]. Further, Pearson correlation analysis demonstrated a positive correlation between UBE2T and FOXA1 (Fig. 4B). JASPAR prediction showed a binding site of UBE2T to FOXA1 in the promoter region of UBE2T (Fig. 4C). Bioinformatics analysis told high FOXA1 expression in LUAD tissues (Fig. 4D), while qRT-PCR and western blot results presented up-regulated FOXA1 level in LUAD cells (Fig. 4E,F). Thereafter, we continued to probe mechanism of influence of FOXA1 and UBE2T on LUAD. As the FOXA1 level in A549 cells was the highest among the tested cell lines, A549 was selected for subsequent experiments. Subsequent ChIP assay showed that FOXA1 antibody could significantly enrich UBE2T compared with IgG (Fig. 4G). The dual luciferase assay found that sh-FOXA1 led to a substantially reduced luciferase activity in UBE2T-WT but caused no great change in the UBE2T-MUT group (Fig. 4H). Finally, the expression of UBE2T in sh-FOXA1-treated A549 cells was assayed by qRT-PCR. UBE2T was significantly down-regulated (Fig. 4I). The above experiments showed that FOXA1 activated UBE2T transcription.

3.5 FOXA1/UBE2T Inhibits CD8⁺T Cell Activity through Glycolysis

To verify the influence of FOXA1/UBE2T on CD8⁺T cell activity in LUAD, we constructed the following cell lines based on A549 cells: sh-NC+oe-NC, sh-FOXA1+oe-NC, and sh-FOXA1+oe-UBE2T. qRT-PCR and MTT were applied for analysis of transfection efficiency and viability of cells respectively. As the results showed, sh-FOXA1 notably impaired UBE2T expression and cell viability of A549, while oe-UBE2T treatment could counteract the effects of sh-FOXA1 on UBE2T expression and cell viability (Fig. 5A,B). According to the results from Seahorse XF extracellular flow analyzer, qRT-PCR and western blot, which detected glycolysis levels and expression of glycolysis-related genes respectively, sh-FOXA1 treated A549 cells had decreased ECAR, increased OCR, and reduced GLUT1, LDHA and HK2 expression; however, oe-UBE2T treatment reversed the above results (Fig. 5C–F). Pyruvate, lactic acid, citric acid, and malic acid contents in cells were tested by corresponding kits, and according to the results, sh-FOXA1 treatment reduced the above indica-

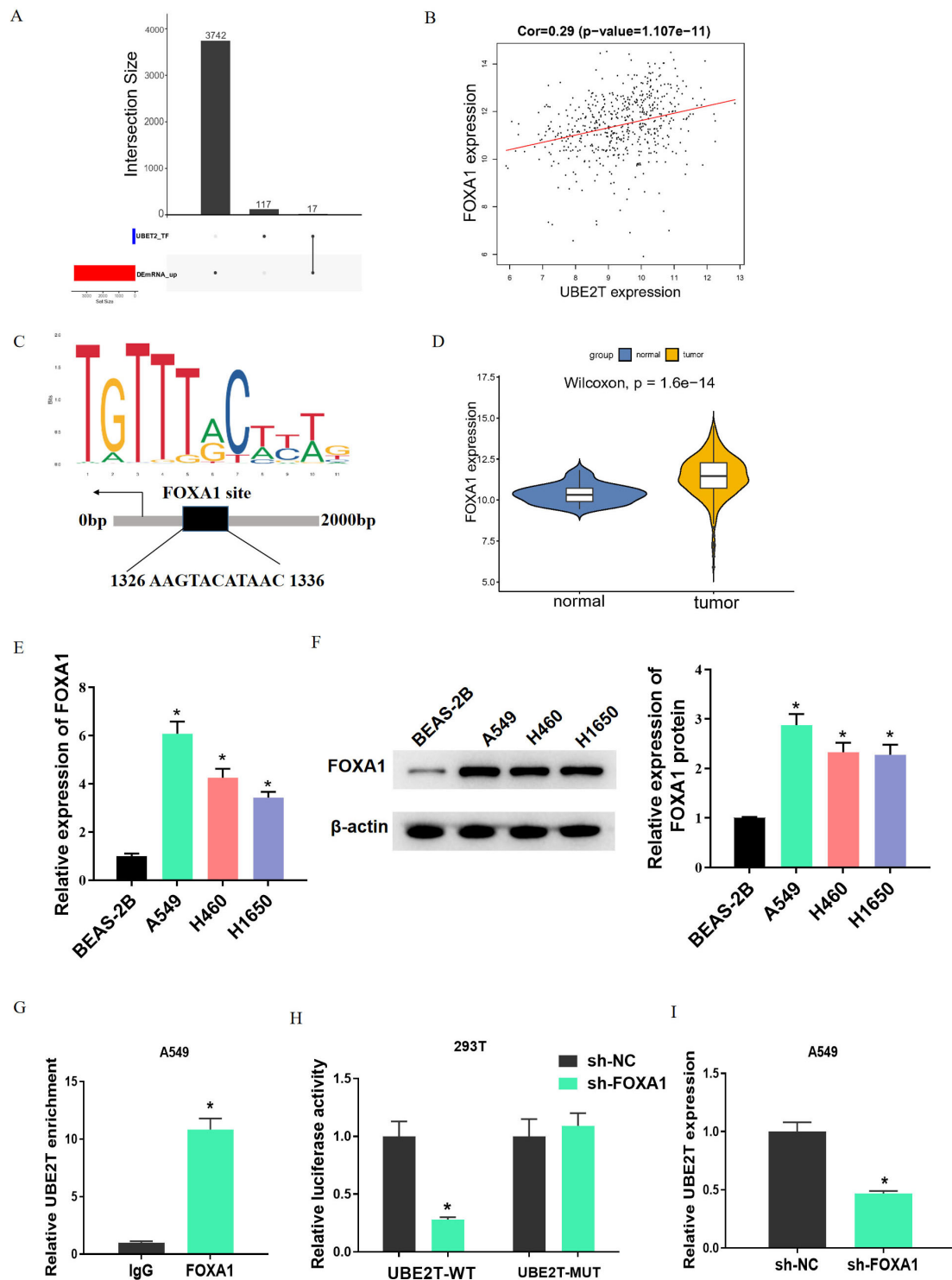


Fig. 4. FOXA1 activates UBE2T transcription. (A) Upset plot of the intersection between hTFtarget predicted transcription factors and up-regulated DEMRNAs. (B) Pearson correlation analysis of UBE2T and FOXA1. (C) JASPAR predicted binding site between UBE2T and FOXA1. (D) FOXA1 expression in LUAD analyzed by bioinformatics means. (E,F) qRT-PCR and western blot results on FOXA1 expression in LUAD cells. (G,H) ChIP and dual luciferase assay results on the binding relationship between UBE2T and FOXA1. (I) qPCR results on UBE2T expression after sh-FOXA1 treatment. * indicates $p < 0.05$. FOXA1, forkhead box A1; ChIP, chromatin immunoprecipitation; hTFtarget, database of human transcription factor targets; DEMRNAs, differentially expressed mRNAs; WT, wild type; MUT, mutation type.

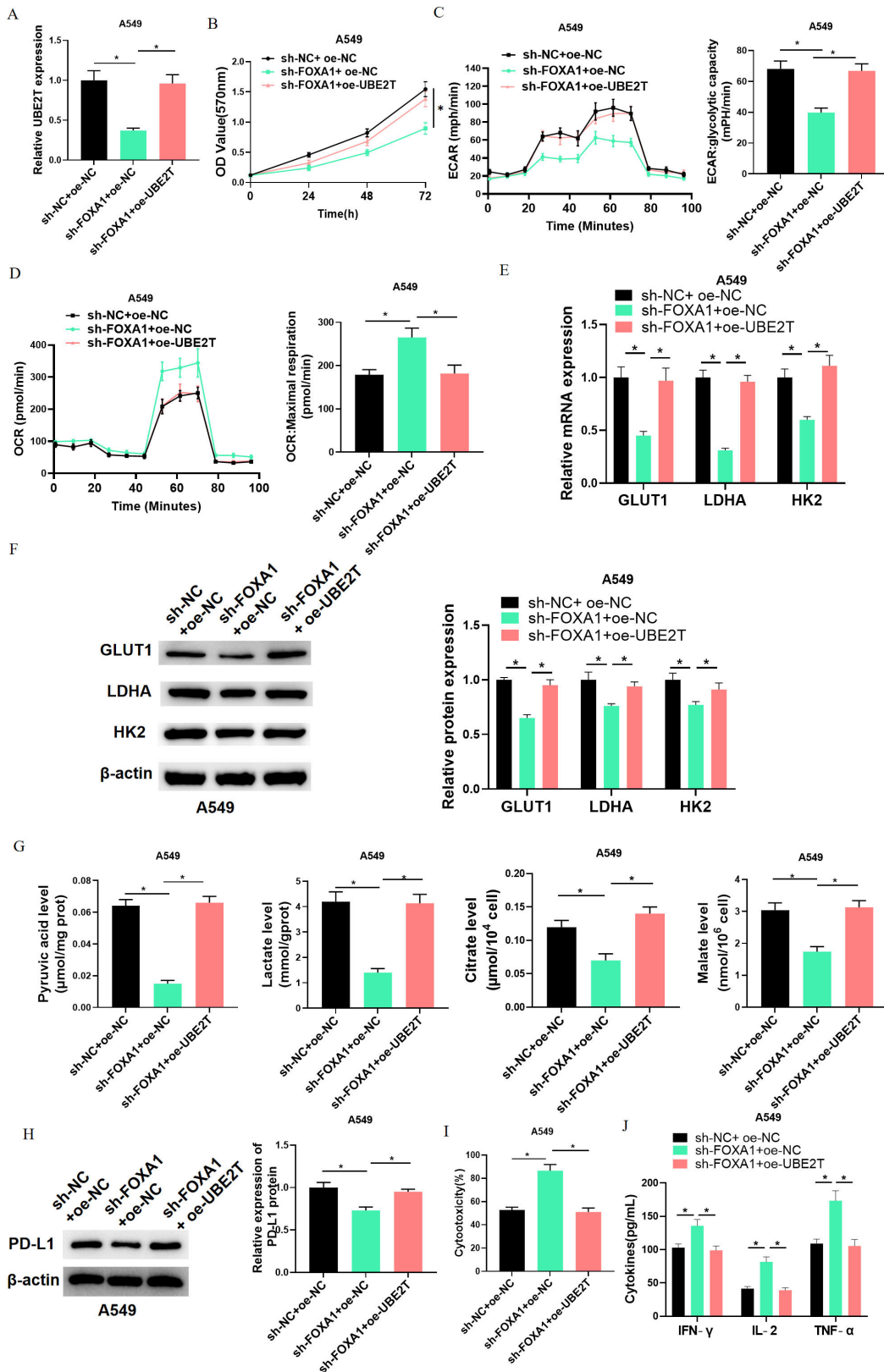


Fig. 5. FOXA1/UBE2T inhibits CD8⁺T cell activity through glycolysis. (A) qRT-PCR detection on transfection efficiency. (B) Cell viability assessed by MTT. (C,D) ECAR and OCR of differently treated cells. (E,F) qRT-PCR and western blot analysis on the expression of glycolysis-related genes after different treatments. (G) Contents of pyruvate, lactic acid, citric acid and malic acid in cells. (H) Western blot results on the expression of PD-L1. (I) CD8⁺T cell cytotoxicity assessed by cytotoxicity assay. (J) ELISA assay results on the expression of cytokines. * indicates $p < 0.05$.

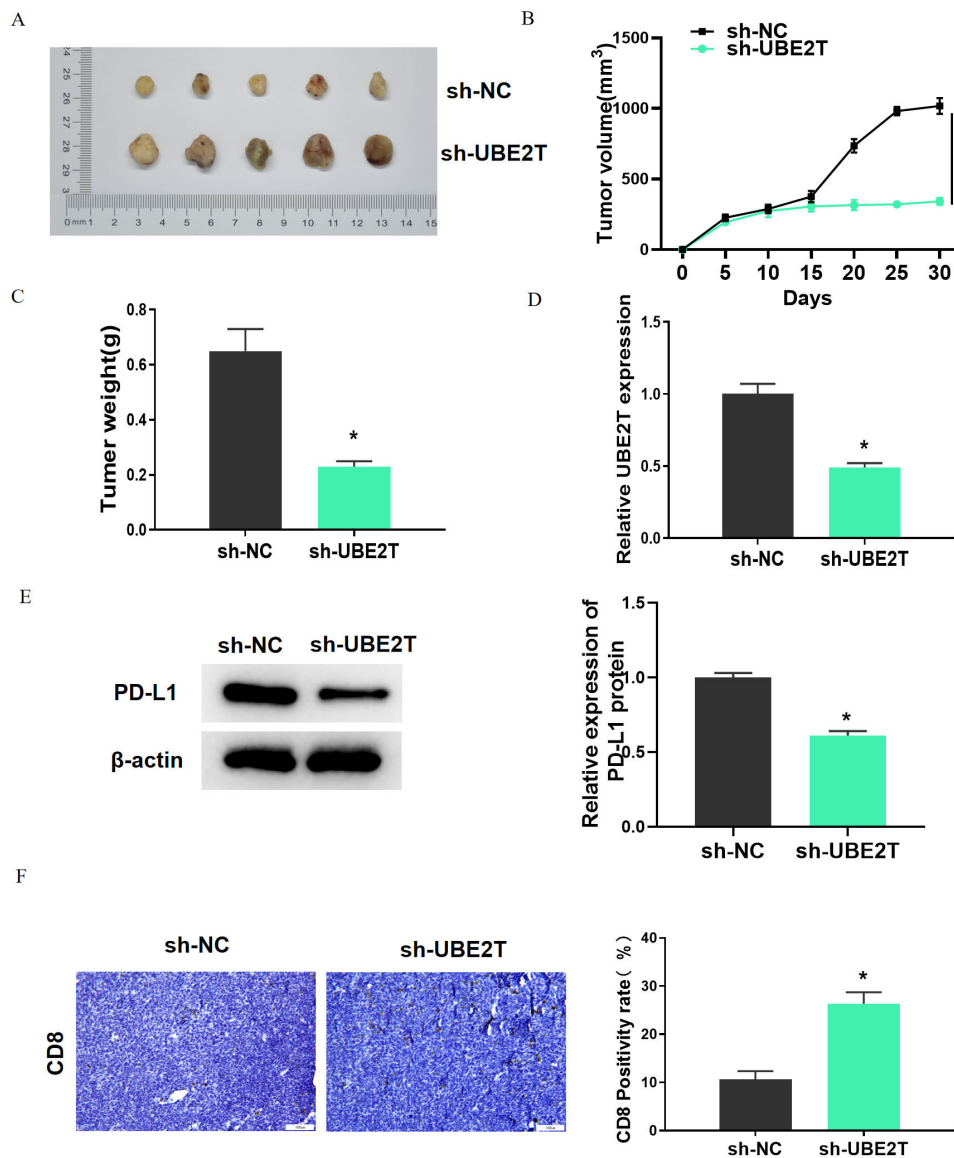


Fig. 6. UBE2T can promote lung adenocarcinoma tumor growth and inhibit CD8⁺T cell infiltration. (A,B) Changes of tumor volume in mice. (C) Effects of different treatments on tumor weight of mice. (D) UBE2T expression detected by qRT-PCR. (E) PD-L1 expression detected by western blot. (F) IHC results on CD8⁺T cell infiltration. * indicates $p < 0.05$. IHC, immunohistochemistry.

tors, but oe-UBE2T counteracted the inhibitory effects of sh-FOXA1 on these indicators (Fig. 5G).

These cells were subjected to co-culture with activated CD8⁺T cells. A549 treated with sh-FOXA1 significantly inhibited PD-L1 expression, promoted CD8⁺T cell cytotoxicity, and elevated expression of IFN- γ , IL-2, and TNF- α , while oe-UBE2T reversed these results (Fig. 5H–J). These results suggested that FOXA1 activated UBE2T expression in LUAD cells and inhibited CD8⁺T cell activity through the glycolysis pathway.

3.6 UBE2T Can Promote LUAD Tumor Growth and Inhibit CD8⁺T Cell Infiltration

We constructed an allograft LUAD model to investigate the tumorigenicity of UBE2T *in vivo*. Compared

with sh-NC, sh-UBE2T had a significant reduction effect on tumor volume and weight (Fig. 6A–C). qRT-PCR, western blot, and IHC analyses showed decreased UBE2T levels and PD-L1 expression after UBE2T knockdown (Fig. 6D,E). According to IHC results, mice treated with sh-UBE2T cells had higher infiltration of CD8⁺T cells than sh-NC group (Fig. 6F). In summary, UBE2T knockdown suppressed tumorigenicity and promoted the immune response of LUAD cells.

4. Discussion

LUAD is a malignancy characterized by uncontrolled cell growth in the lungs and bronchus [37]. Currently, the treatment methods of LUAD are mainly surgical re-

section, chemotherapy, radiotherapy, and targeted therapy, but the clinical outcomes are unsatisfactory due to the lack of reliable biomarkers [38]. Hence, an effective molecular marker is in need to project early onset of LUAD and formulate therapies. Recently, immunotherapy targeting immune checkpoints has shown great promise in cancer treatment, and immune escape is the biggest obstacle to effective cancer treatment [39]. However, the molecular mechanism of immune escape of LUAD has not been perfected. Hence, this study aimed to search for new biomarkers as a theoretical basis for new therapies for LUAD.

UBE2T is an oncogene whose up-regulated expression has been noticed in many kinds of cancer. Moreover, the carcinogenic effect of UBE2T in LUAD has also been demonstrated. For example, UBE2T is up-regulated in LUAD, targeted by NEDD4, and inhibits PI3K-AKT signal through ubiquitination and degradation, which collectively lead to LUAD progression [40]. As Zhu *et al.* [18] found, UBE2T overexpression could promote the proliferation of LUAD cells and autophagy triggered by cisplatin, resulting in cisplatin resistance of A549 cells. Here we also found an aberrant high UBE2T expression in LUAD, which is in line with previous studies. Additionally, UBE2T participates in metabolic reprogramming during the development of cancer. For example, UBE2T features in promoting tumor cell proliferation, invasion, and glycolysis via PI3K/AKT pathway in breast cancer [29]. Through bioinformatics analysis, we know that a high UBE2T level in LUAD could activate glycolysis signaling pathways. This suggests that UBE2T affecting the progression of LUAD through glycolysis is one of the mechanisms. UBE2T has a potentially pivotal role in LUAD progression.

Immune escape is a critical pathway to avoid T cell-mediated specific immune killing for tumor cells in the TME [32]. A diet low in glucose enhances the host lung immune responses and hinders the formation of tumors in experimental lung adenocarcinomas [41]. Cancer cells undergo a high glucose consumption and lactic acid production during the reprogramming of glucose metabolism, which leaves the TME deficient in oxygen and energy. This has a significant effect on immunity and helps cancer cells evade immune surveillance [15]. Guo *et al.* [42] discovered that in human glioblastoma cells, aerobic glycolysis mediated by hexokinase 2 (HK2) upregulates PD-L1 via phosphorylation of $I\kappa B\alpha$, leading to reduced infiltration of CD8⁺T cells and facilitating tumor immune evasion. In this work, overexpression of UBE2T in LUAD activated the glycolysis pathway, up-regulated key glycolytic enzymes HK2, LDHA and GLUT1, and repressed the activity of CD8⁺T cells by promoting PD-L1 expression, thus promoting immune escape of LUAD. Taken together with previous studies, we hypothesized that it may be UBE2T that regulated HK2 expression, leading to $I\kappa B\alpha$ phosphorylation, $I\kappa B\alpha$ degradation and NF- κ B activation, which up-regulated PD-L1 and thus had an effect on CD8⁺T cell ac-

tivity. In a word, UBE2T might drive immune evasion of LUAD via activation of glycolysis, thus promoting malignant progression of LUAD.

We also found that FOXA1 was the upstream transcription factor for UBE2T, and UBE2T expression was positively regulated by this factor. FOXA1 has been reported to regulate cancer development by activating target genes. For example, FOXA1 can act with the promoter of TGFB3 and inhibit its accumulation in the nuclear; miR-93-5p can reduce FOXA1 expression and elevate TGFB3 expression; thus, apoptosis of colorectal cancer cells is inhibited [43]. FOXA1 promotes cell cycle progression in chondrosarcoma cells by activating the cyclin B1 expression [44]. A clinical study showed that adjuvant endocrine therapy is implicated in FOXA1 downregulation in pleural metastases [45]. FOXA1 intimately participates in production and function of regulatory T cells (Tregs). Liang *et al.* [46] demonstrated that FOXA1 Tregs are enhanced in lung cancer and suppress anti-tumor immunity of T cells. In the current study, we found through bioinformatic analysis that FOXA1 was a transcription factor for UBE2T. By binding to UBE2T promoter, FOXA1 targeted UBE2T expression and promoted LUAD immune escape by activating the glycolysis pathway.

However, our experiment was conducted only at the cellular and animal levels, and the repeated experimental results were not collected from clinical LUAD patients, which is a limitation. In addition, specific molecular mechanism of UBE2T activation of aerobic glycolysis affecting activity of CD8⁺T cells to regulate tumor immune evasion still requires further research. We proceed to verify the findings by collecting clinical tissues.

5. Conclusion

Collectively, according to our results, UBE2T was significantly overexpressed in LUAD; UBE2T expression was positively regulated by FOXA1, and UBE2T up-regulated PD-L1 expression by activating glycolytic metabolism, thus inhibiting CD8⁺T activity, leading to LUAD immune escape. Our results suggested FOXA1/UBE2T as a potential target for immunotherapy of LUAD. In conclusion, our findings proffered a new view for understanding the progression of LUAD and suggested FOXA1/UBE2T as a prospective target for LUAD therapy.

Availability of Data and Materials

The data and materials in the current study are available from the corresponding author on reasonable request.

Author Contributions

Conceptualization: JP. Visualization: KW and BW. Acquiring: ZY. Analyzing: QS and DZ. Interpreting data: PZ, WY and ZY. Resources: DZ. Writing - Original Draft: KW, ZY, JP and DZ. Writing - Review & Editing: QS,

PZ, BW and WY. All authors read and approved the final manuscript. All authors have participated sufficiently in the work and agreed to be accountable for all aspects of the work.

Ethics Approval and Consent to Participate

The animal experiments in this study were performed with the approval from the Ethics Committee of Affiliated Hospital of Southwest Medical University (No. 20221206-007).

Acknowledgment

Not applicable.

Funding

This research received no external funding.

Conflict of Interest

The authors declare no conflict of interest.

Supplementary Material

Supplementary material associated with this article can be found, in the online version, at <https://doi.org/10.31083/j.fbl2904134>.

References

- [1] Xing Y, Luo P, Hu R, Wang D, Zhou G, Jiang J. TRIB3 Promotes Lung Adenocarcinoma Progression via an Enhanced Warburg Effect. *Cancer Management and Research*. 2020; 12: 13195–13206.
- [2] Ling B, Liao X, Tang Q, Ye G, Bin X, Wang J, *et al.* MicroRNA-106b-5p inhibits growth and progression of lung adenocarcinoma cells by downregulating IGSF10. *Aging*. 2021; 13: 18740–18756.
- [3] Wang J, Zhao X, Wang Y, Ren F, Sun D, Yan Y, *et al.* circRNA-002178 act as a ceRNA to promote PDL1/PD1 expression in lung adenocarcinoma. *Cell Death & Disease*. 2020; 11: 32.
- [4] Dai X, Lu L, Deng S, Meng J, Wan C, Huang J, *et al.* USP7 targeting modulates anti-tumor immune response by reprogramming Tumor-associated Macrophages in Lung Cancer. *Theranostics*. 2020; 10: 9332–9347.
- [5] Jiang X, Wang J, Deng X, Xiong F, Ge J, Xiang B, *et al.* Role of the tumor microenvironment in PD-L1/PD-1-mediated tumor immune escape. *Molecular Cancer*. 2019; 18: 10.
- [6] Wu Y, Chen W, Xu ZP, Gu W. PD-L1 Distribution and Perspective for Cancer Immunotherapy-Blockade, Knockdown, or Inhibition. *Frontiers in Immunology*. 2019; 10: 2022.
- [7] Liu Z, Wang T, She Y, Wu K, Gu S, Li L, *et al.* N⁶-methyladenosine-modified circIGF2BP3 inhibits CD8⁺ T-cell responses to facilitate tumor immune evasion by promoting the deubiquitination of PD-L1 in non-small cell lung cancer. *Molecular Cancer*. 2021; 20: 105.
- [8] Yang J, Jia Y, Wang B, Yang S, Du K, Luo Y, *et al.* Circular RNA CHST15 Sponges miR-155-5p and miR-194-5p to Promote the Immune Escape of Lung Cancer Cells Mediated by PD-L1. *Frontiers in Oncology*. 2021; 11: 595609.
- [9] Bian XL, Chen HZ, Yang PB, Li YP, Zhang FN, Zhang JY, *et al.* Nur77 suppresses hepatocellular carcinoma via switching glucose metabolism toward gluconeogenesis through attenuating phosphoenolpyruvate carboxykinase sumoylation. *Nature Communications*. 2017; 8: 14420.
- [10] Li W, Xu M, Li Y, Huang Z, Zhou J, Zhao Q, *et al.* Comprehensive analysis of the association between tumor glycolysis and immune/inflammation function in breast cancer. *Journal of Translational Medicine*. 2020; 18: 92.
- [11] Li C, Zhang G, Zhao L, Ma Z, Chen H. Metabolic reprogramming in cancer cells: glycolysis, glutaminolysis, and Bcl-2 proteins as novel therapeutic targets for cancer. *World Journal of Surgical Oncology*. 2016; 14: 15.
- [12] Fang Z, Sun Q, Yang H, Zheng J. SDHB Suppresses the Tumorigenesis and Development of ccRCC by Inhibiting Glycolysis. *Frontiers in Oncology*. 2021; 11: 639408.
- [13] Zhao S, Guan B, Mi Y, Shi D, Wei P, Gu Y, *et al.* LncRNA MIR17HG promotes colorectal cancer liver metastasis by mediating a glycolysis-associated positive feedback circuit. *Oncogene*. 2021; 40: 4709–4724.
- [14] Yu Y, Liang Y, Li D, Wang L, Liang Z, Chen Y, *et al.* Glucose metabolism involved in PD-L1-mediated immune escape in the malignant kidney tumour microenvironment. *Cell Death Discovery*. 2021; 7: 15.
- [15] Zhang Q, Liu J, Lin H, Lin B, Zhu M, Li M. Glucose metabolism reprogramming promotes immune escape of hepatocellular carcinoma cells. *Exploration of Targeted Anti-tumor Therapy*. 2023; 4: 519–536.
- [16] Xiang H, Yang R, Tu J, Xi Y, Yang S, Lv L, *et al.* Metabolic reprogramming of immune cells in pancreatic cancer progression. *Biomedicine & Pharmacotherapy = Biomedecine & Pharmacotherapie*. 2023; 157: 113992.
- [17] Duan Q, Li H, Gao C, Zhao H, Wu S, Wu H, *et al.* High glucose promotes pancreatic cancer cells to escape from immune surveillance via AMPK-Bmi1-GATA2-MICA/B pathway. *Journal of Experimental & Clinical Cancer Research: CR*. 2019; 38: 192.
- [18] Zhu J, Ao H, Liu M, Cao K, Ma J. UBE2T promotes autophagy via the p53/AMPK/mTOR signaling pathway in lung adenocarcinoma. *Journal of Translational Medicine*. 2021; 19: 374.
- [19] Tao Y, Li R, Shen C, Li J, Zhang Q, Ma Z, *et al.* SENP1 is a crucial promoter for hepatocellular carcinoma through deSUMOylation of UBE2T. *Aging*. 2020; 12: 1563–1576.
- [20] Luo C, Yao Y, Yu Z, Zhou H, Guo L, Zhang J, *et al.* UBE2T knockdown inhibits gastric cancer progression. *Oncotarget*. 2017; 8: 32639–32654.
- [21] Zhang W, Zhang Y, Yang Z, Liu X, Yang P, Wang J, *et al.* High expression of UBE2T predicts poor prognosis and survival in multiple myeloma. *Cancer Gene Therapy*. 2019; 26: 347–355.
- [22] Yin H, Wang X, Zhang X, Zeng Y, Xu Q, Wang W, *et al.* UBE2T promotes radiation resistance in non-small cell lung cancer via inducing epithelial-mesenchymal transition and the ubiquitination-mediated FOXO1 degradation. *Cancer Letters*. 2020; 494: 121–131.
- [23] Wang Z, Chen N, Liu C, Cao G, Ji Y, Yang W, *et al.* UBE2T is a prognostic biomarker and correlated with Th2 cell infiltrates in retinoblastoma. *Biochemical and Biophysical Research Communications*. 2022; 614: 138–144.
- [24] Xiao Y, Deng Z, Li Y, Wei B, Chen X, Zhao Z, *et al.* ANLN and UBE2T are prognostic biomarkers associated with immune regulation in breast cancer: a bioinformatics analysis. *Cancer Cell International*. 2022; 22: 193.
- [25] Zhang Y, Huang YX, Wang DL, Yang B, Yan HY, Lin LH, *et al.* LncRNA DSCAM-AS1 interacts with YBX1 to promote cancer progression by forming a positive feedback loop that activates FOXA1 transcription network. *Theranostics*. 2020; 10: 10823–10837.
- [26] Arruabarrena-Aristorena A, Maag JLV, Kittane S, Cai Y, Karthaus WR, Ladewig E, *et al.* FOXA1 Mutations Reveal Dis-

- tinct Chromatin Profiles and Influence Therapeutic Response in Breast Cancer. *Cancer Cell*. 2020; 38: 534–550.e9.
- [27] Pomerantz MM, Li F, Takeda DY, Lenci R, Chonkar A, Chabot M, *et al*. The androgen receptor cistrome is extensively reprogrammed in human prostate tumorigenesis. *Nature Genetics*. 2015; 47: 1346–1351.
- [28] Wang X, Yin Y, Du R. SOX9 dependent FOXA1 expression promotes tumorigenesis in lung carcinoma. *Biochemical and Biophysical Research Communications*. 2019; 516: 236–244.
- [29] Qiao L, Dong C, Ma B. UBE2T promotes proliferation, invasion and glycolysis of breast cancer cells by regulating the PI3K/AKT signaling pathway. *Journal of Receptor and Signal Transduction Research*. 2022; 42: 151–159.
- [30] Zhou C, Wei W, Ma J, Yang Y, Liang L, Zhang Y, *et al*. Cancer-secreted exosomal miR-1468-5p promotes tumor immune escape via the immunosuppressive reprogramming of lymphatic vessels. *Molecular Therapy: the Journal of the American Society of Gene Therapy*. 2021; 29: 1512–1528.
- [31] Chen Y, Feng Z, Kuang X, Zhao P, Chen B, Fang Q, *et al*. Increased lactate in AML blasts upregulates TOX expression, leading to exhaustion of CD8⁺ cytolytic T cells. *American Journal of Cancer Research*. 2021; 11: 5726–5742.
- [32] Tian P, Wei JX, Li J, Ren JK, Yang JJ. LncRNA SNHG1 regulates immune escape of renal cell carcinoma by targeting miR-129-3p to activate STAT3 and PD-L1. *Cell Biology International*. 2021; 45: 1546–1560.
- [33] Ma G, Chen J, Wei T, Wang J, Chen W. Inhibiting roles of FOXA2 in liver cancer cell migration and invasion by transcriptionally suppressing microRNA-103a-3p and activating the GREM2/LATS2/YAP axis. *Cytotechnology*. 2021; 73: 523–537.
- [34] Sun J, Zhu Z, Li W, Shen M, Cao C, Sun Q, *et al*. UBE2T-regulated H2AX monoubiquitination induces hepatocellular carcinoma radioresistance by facilitating CHK1 activation. *Journal of Experimental & Clinical Cancer Research: CR*. 2020; 39: 222.
- [35] Wang X, Liu Y, Leng X, Cao K, Sun W, Zhu J, *et al*. UBE2T Contributes to the Prognosis of Esophageal Squamous Cell Carcinoma. *Pathology Oncology Research: POR*. 2021; 27: 632531.
- [36] Orstad G, Fort G, Parnell TJ, Jones A, Stubben C, Lohman B, *et al*. FoxA1 and FoxA2 control growth and cellular identity in NKX2-1-positive lung adenocarcinoma. *Developmental Cell*. 2022; 57: 1866–1882.e10.
- [37] Yu Y, Wang Z, Zheng Q, Li J. GREB1L overexpression correlates with prognosis and immune cell infiltration in lung adenocarcinoma. *Scientific Reports*. 2021; 11: 13281.
- [38] Yao Y, Zhou Y, Hua Q. circRNA hsa_circ_0018414 inhibits the progression of LUAD by sponging miR-6807-3p and upregulating DKK1. *Molecular Therapy. Nucleic Acids*. 2021; 23: 783–796.
- [39] Chen Z, Huang Y, Hu Z, Zhao M, Li M, Bi G, *et al*. Landscape and dynamics of single tumor and immune cells in early and advanced-stage lung adenocarcinoma. *Clinical and Translational Medicine*. 2021; 11: e350.
- [40] Chen Y, Hong H, Wang Q, Li J, Zhang W, Chen T, *et al*. NEDD4L-induced ubiquitination mediating UBE2T degradation inhibits progression of lung adenocarcinoma via PI3K-AKT signaling. *Cancer Cell International*. 2021; 21: 631.
- [41] Gähler A, Trufa DI, Chiriac MT, Tausche P, Hohenberger K, Brunst AK, *et al*. Glucose-Restricted Diet Regulates the Tumor Immune Microenvironment and Prevents Tumor Growth in Lung Adenocarcinoma. *Frontiers in Oncology*. 2022; 12: 873293.
- [42] Guo D, Tong Y, Jiang X, Meng Y, Jiang H, Du L, *et al*. Aerobic glycolysis promotes tumor immune evasion by hexokinase2-mediated phosphorylation of IκBα. *Cell Metabolism*. 2022; 34: 1312–1324.e6.
- [43] Chen X, Liu J, Zhang Q, Liu B, Cheng Y, Zhang Y, *et al*. Exosome-mediated transfer of miR-93-5p from cancer-associated fibroblasts confer radioresistance in colorectal cancer cells by downregulating FOXA1 and upregulating TGFB3. *Journal of Experimental & Clinical Cancer Research: CR*. 2020; 39: 65.
- [44] Lin ZS, Chung CC, Liu YC, Chen TM, Yu YL, Wang SC, *et al*. FOXA1 transcriptionally up-regulates cyclin B1 expression to enhance chondrosarcoma progression. *American Journal of Cancer Research*. 2018; 8: 1989–2004.
- [45] Schrijver W, Schuurman K, van Rossum A, Droog M, Jeronimo C, Salta S, *et al*. FOXA1 levels are decreased in pleural breast cancer metastases after adjuvant endocrine therapy, and this is associated with poor outcome. *Molecular Oncology*. 2018; 12: 1884–1894.
- [46] Liang J, Tian C, Zeng Y, Yang Q, Liu Y, Liu Y, *et al*. FOXA1⁺ regulatory T cells: A novel T cell subset that suppresses anti-tumor immunity in lung cancer. *Biochemical and Biophysical Research Communications*. 2019; 514: 308–315.